Loss of Vac14, a regulator of the signaling lipid phosphatidylinositol 3,5-bisphosphate, results in neurodegeneration in mice

Yanling Zhang*†, Sergey N. Zolov*, Clement Y. Chow‡, Shalom G. Slutsky§, Simon C. Richardson¶, Robert C. Piper¶, Baoli Yang‖, Johnathan J. Nau†, Randal J. Westrick‡, Sean J. Morrison§, Miriam H. Meisler‡, and Lois S. Weisman*,**††

*Life Sciences Institute, ‡Department of Human Genetics, **Department of Cellular and Developmental Biology, and §Howard Hughes Medical Institute and Department of Internal Medicine and Center for Stem Cell Biology, University of Michigan, Ann Arbor, MI 48109; and Departments of †Biochemistry, ¶Physiology, and ‖Obstetrics and Gynecology, University of Iowa, Iowa City, IA 52242

Edited by Pietro V. De Camilli, Yale University School of Medicine, New Haven, CT, and approved September 17, 2007 (received for review March 12, 2007)

The signaling lipid, phosphatidylinositol 3,5-bisphosphate ($PI(3,5)P_2$), likely functions in multiple signaling pathways. Here, we report the characterization of a mouse mutant lacking Vac14, a regulator of $PI(3,5)P_2$ synthesis. The mutant mice exhibit massive neurodegeneration, particularly in the midbrain and in peripheral sensory neurons. Cell bodies of affected neurons are vacuolated, and apparently empty spaces are present in areas where neurons should be present. Similar vacuoles are found in cultured neurons and fibroblasts. Selective membrane trafficking pathways, especially endosome-to-TGN retrograde trafficking, are defective. This report, along with a recent report on a mouse with a null mutation in *Fig4*, presents the unexpected finding that the housekeeping lipid, $PI(3,5)P_2$, is critical for the survival of neural cells.

Fab1 | PIKfyve | $PtdIns(3,5)P_2$ | spongiform | endosomal traffic

The low-abundance signaling lipids, phosphatidylinositol 3,5-bisphosphate ($PI(3,5)P_2$) and phosphatidylinositol 5-phosphate (PI(5)P), were discovered relatively recently (1–3). Because of their low abundance and the limited number of tools available for their study, relatively little is known about these lipids.

An interesting property of $PI(3,5)P_2$ occurs in yeast, where a stimulus of hyperosmotic shock induces dramatic and transient changes in the levels of $PI(3,5)P_2$. The levels of $PI(3,5)P_2$ transiently rise >20-fold (4). Within 1 minute, the levels rise 5-fold; by 5 minutes, they increase >20-fold; there is a short plateau of 10 min, and then $PI(3,5)P_2$ levels decrease at a rate similar to their increase. The rapid decrease in $PI(3,5)P_2$ levels occurs even though the cells remain in hyperosmotic media. Vacuole volume undergoes transient changes that parallel $PI(3,5)P_2$ levels. That these rapid and transient changes occur even in the presence of a sustained stimulus strongly suggests that $PI(3,5)P_2$ plays a major role in signaling pathways related to adaptation.

Several proteins are required for the synthesis and turnover of $PI(3,5)P_2$. $PI(3,5)P_2$ is synthesized from PI(3)P by the PI(3)P 5-kinase Fab1/PIKfyve/PIP5K3 (5, 6). Fab1 is stimulated by a regulatory complex that contains Vac14 (7, 8) and Fig4 (4, 9). Surprisingly, the Vac14/Fig4 complex plays two opposing roles in the regulation of steady-state levels of $PI(3,5)P_2$. Vac14/Fig4 both activate Fab1 and also function in the breakdown of $PI(3,5)P_2$ through the lipid phosphatase activity of Fig4 (4, 9–11).

In mammals, generation of $PI(3,5)P_2$ is predicted to impact PI(5)P production. *In vitro* studies have shown that PI(5)P can be generated from $PI(3,5)P_2$ through the $PI(3,5)P_2$ 3-phosphatase activity of members of the myotubularin family and related proteins including MTM1, MTMR1, MTMR2, MTMR3, MTMR6, and hJUMPY/MTMR14 (12–15). In addition, PIKfyve/Fab1 can generate both $PI(3,5)P_2$ and PI(5)P *in vitro* (16). The source of PI(5)P *in vivo* has not been established. However, the generation of PI(5)P from either pathway requires PIKfyve/Fab1 activity, either to produce the substrate for myotubularin [$PI(3,5)P_2$] or to produce PI(5)P directly from PI.

Haploinsufficiency of human Fab1/PIP5K3 is associated with Francois–Neetens mouchetée corneal fleck dystrophy, a mild syndrome characterized by vacuoles in the cornea (17). Because one normal Fab1/PIP5K3 allele is present, affected individuals likely retain the ability to synthesize $PI(3,5)P_2$ and PI(5)P. Thus, the physiological effect of depletion of these lipids in mammals was not known. To determine the physiological functions of $PI(3,5)P_2$ in mammals, we characterized a mouse mutant deficient in the Fab1 regulator, Vac14. We chose Vac14 rather than Fab1 because, in yeast, *vac14* but not *fab1* mutants maintain a low level of $PI(3,5)P_2$, and *vac14* mutants have a less severe growth defect. The yeast studies led to the prediction that loss of Vac14 in mammals might result in a milder defect than loss of Fab1.

Results

The embryonic stem cell clone RRP155 obtained from the University of California Bay Genomics repository (San Francisco, CA) contains a β-geo gene-trap vector inserted into intron 1 of Vac14 [supporting information (SI) Fig. 6 *a* and *b*]. Chimeric mice were crossed with C57BL/6J wild-type mice. Offspring with germ-line transmission of the Vac14-β-geo allele were obtained. Heterozygous mice appeared normal. Just after birth [postnatal day (P)0] homozygous $Vac14^{\beta\text{-geo}/\beta\text{-geo}}$ pups appeared normal externally and were similar in size to their wild-type and $Vac14^{+/\beta\text{-geo}}$ littermates (SI Fig. 6*c*). From midgestation through P0, we observed 39 homozygous mutants among 167 total animals, a value consistent with the Mendelian prediction of 25%, ($P = 0.78$ by the χ^2 test) (SI Table 1). All $Vac14^{\beta\text{-geo}/\beta\text{-geo}}$ mice died within 1–2 days after birth.

To test whether Vac14 protein was produced in the $Vac14^{\beta\text{-geo}/\beta\text{-geo}}$ mutants, extracts from mouse primary fibroblasts were tested by Western blot analysis using polyclonal antibodies raised to human full-length Vac14. The antibody recognizes both

Author contributions: Y.Z. and S.N.Z. contributed equally to this work; Y.Z., S.N.Z., S.G.S., S.J.M., and L.S.W. designed research; Y.Z., S.N.Z., S.G.S., B.Y., and J.J.N. performed research; C.Y.C., S.C.R., R.C.P., J.J.N., R.J.W., and M.H.M. contributed new reagents/analytic tools; Y.Z., S.N.Z., S.G.S., S.J.M., and L.S.W. analyzed data; and Y.Z., S.N.Z., S.G.S., and L.S.W. wrote the paper.

The authors declare no conflict of interest.

This article is a PNAS Direct Submission.

Freely available online through the PNAS open access option.

Abbreviations: CI-MPR, cation-independent mannose-6-phosphate receptor; P(*n*), postnatal day (*n*); $PI(3,5)P_2$, phosphatidylinositol 3,5-bisphosphate; PI(5)P, PI 5-phosphate;

††To whom correspondence should be addressed at: Life Sciences Institute, 210 Washtenaw Avenue, Room 6437, University of Michigan, Ann Arbor, MI 48109-2216. E-mail: lweisman@umich.edu.

This article contains supporting information online at www.pnas.org/cgi/content/full/0702275104/DC1.

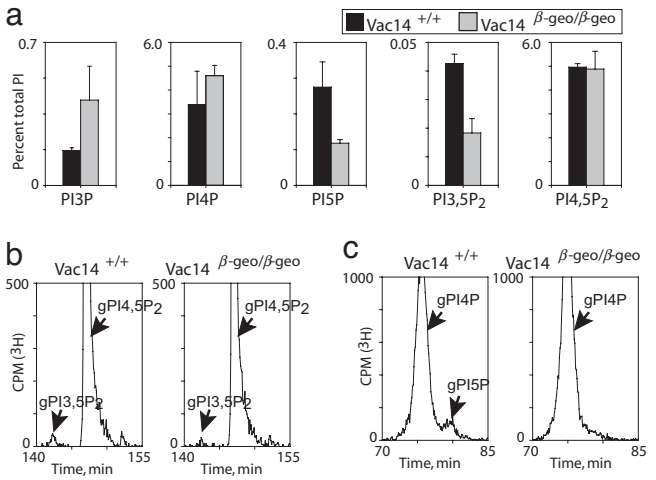

Fig. 1. The Vac14$^{\beta\text{-geo}/\beta\text{-geo}}$ mouse has no detectable Vac14 protein and has a decrease in PI(3,5)P_2 and PI(5)P levels. (*a*) PI(3,5)P_2 and PI(5)P levels decrease, whereas PI(3)P levels increase in Vac14$^{\beta\text{-geo}/\beta\text{-geo}}$ mice. Primary fibroblasts were starved in inositol-free DMEM for 12 h and labeled with *myo*-[2-^{3}H]inositol for 24 h. Lipids were extracted, deacylated, and analyzed by anion-exchange HPLC chromatography. To assess whether differences in the lipid levels were statistically significant, we applied a two-tailed, paired Student's *t* test. Significance was set at $P = 0.15$. PI(3)P increased ($P = 0.11$), whereas PI(3,5)P_2 and PI(5)P decreased in Vac14$^{\beta\text{-geo}/\beta\text{-geo}}$ cells ($P = 0.0070$ and 0.0038, respectively). PI(4)P and PI(4,5)P_2 levels did not change ($P = 0.36$ and 0.87, respectively). For all measurements, $n = 3$. Error bars represent the standard deviations. (*b* and *c*) Regions of HPLC profiles showing PI(3,5)P_2 (*b*) and PI(5)P (*c*) from Vac14$^{+/+}$ (*Left*) and Vac14$^{\beta\text{-geo}/\beta\text{-geo}}$ (*Right*).

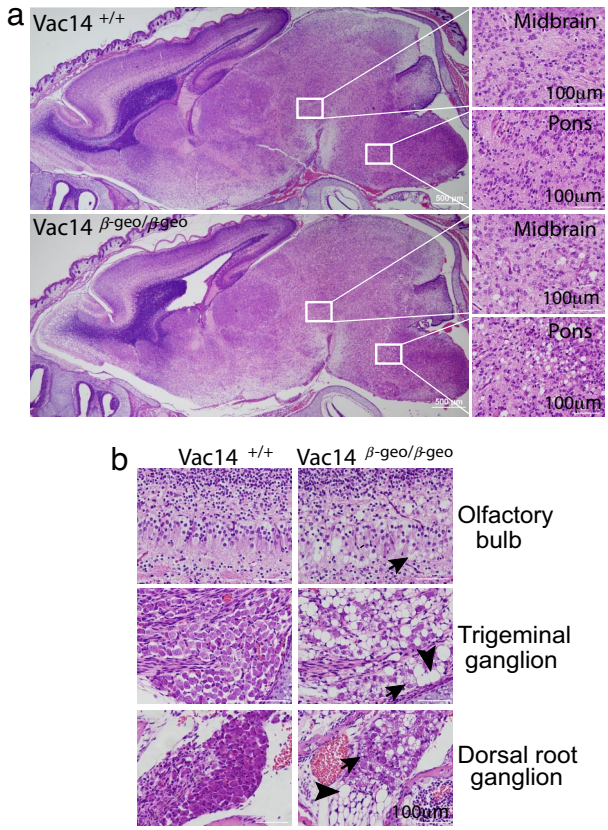

Fig. 2. Lesions in neural tissue from Vac14$^{\beta\text{-geo}/\beta\text{-geo}}$ mutant mice. (*a*) Sagittal sections of the whole brain of P0 mice. Examples of lesions (holes) in affected regions, midbrain (*Upper*) and pons (*Lower*), are shown on the right with higher magnification. (Scale bars, 100 μm.) *Insets* are also indicated by the squares in the whole brain. (*b*) Lesions composed of large intracellular vacuoles (arrows) or acellular areas were found in olfactory bulb, trigeminal ganglion, and dorsal root ganglion. In some cases, whole cell bodies appeared to be either missing or filled with one giant vacuole (arrowheads). (Scale bars, 100 μm.)

human and mouse Vac14. No Vac14 protein was detected in the Vac14$^{\beta\text{-geo}/\beta\text{-geo}}$ extracts (SI Fig. 6*d*). In addition, the levels of Fab1 are normal in both Vac14$^{\beta\text{-geo}/\beta\text{-geo}}$ brains and cultured fibroblasts (SI Fig. 6 *d* and *e*). Thus, the phenotypes observed in the Vac14$^{\beta\text{-geo}/\beta\text{-geo}}$ mouse are likely because of the absence of Vac14 protein.

In wild-type mice, Vac14 and Fab1 proteins were expressed in all tissues examined (SI Fig. 6*e*). This finding, along with the observation that these conserved proteins serve housekeeping functions in yeast, suggested that PI(3,5)P_2 and/or PI(5)P, are required in all tissues.

Knockout of Vac14 in yeast is deleterious and results in abnormally low levels of PI(3,5)P_2 (4, 9). To test the role of Vac14 in the maintenance of steady-state levels of phosphoinositide polyphosphates in mammalian cells, we cultured fibroblasts from wild-type and Vac14$^{\beta\text{-geo}/\beta\text{-geo}}$ P0 animals and measured the levels of these lipids. In yeast, PI(3,5)P_2 is a very low-abundance lipid; ≈0.08% of the total PI in the cell (4). In wild-type mouse fibroblasts, the levels of PI(3,5)P_2 are even lower; 0.04 ± 0.003% of the total PI. PI(3,5)P_2 levels were significantly reduced in the Vac14$^{\beta\text{-geo}/\beta\text{-geo}}$ mutant, 0.02 ± 0.005% (Fig. 1 *a* and *b*). Thus, in mammals, Vac14 has a key role in the maintenance of steady-state levels of PI(3,5)P_2. Consistent with a defect in the synthesis of PI(3,5)P_2, the level of PI(3)P was elevated in Vac14$^{\beta\text{-geo}/\beta\text{-geo}}$ fibroblasts; 0.5 ± 0.2% in the mutant vs. 0.2 ± 0.02% in wild type. Based on studies in yeast (4, 7, 9), we postulate that the elevated pool of PI(3)P represents substrate that would normally be consumed by the PI(3)P 5-kinase Fab1. Because of the absence of Vac14, Fab1 is not properly activated, and thus its substrate accumulates. The levels of PI(5)P were also significantly reduced; 0.3 ± 0.07% in wild type vs. 0.1 ± 0.005% in the mutant (Fig. 1 *a* and *c*). The lower level of PI(5)P may be due either to reduction in Fab1 kinase activity or to reduction of PI(3,5)P_2, the substrate for the 3-phosphatase activity of myotubularins. Neither PI(3,4)P_2 nor PI(3,4,5)P_3 was detected in the wild-type or mutant fibroblasts. The levels of these lipids are generally exceedingly low and often cannot be detected unless cells are stimulated, for example, with PDGF (1, 18). The above analysis of phosphatidylinositol polyphosphates in primary fibroblasts strongly suggests that, in mammals, Vac14 is required to maintain normal levels of PI(3)P, PI(3,5)P_2, and PI(5)P.

To further characterize phenotypes associated with loss of Vac14, sagittal sections of P0 pups were stained with H&E (Fig. 2*a*). Profound defects were observed in the nervous system. Most notable were lesions in several regions of the Vac14$^{\beta\text{-geo}/\beta\text{-geo}}$ brain, including the preoptic area, thalamus, hypothalamus (SI Table 2). Other regions including the hippocampus and the cortex were less affected (SI Fig. 7*a* and SI Table 2). The lesions appeared to be either neuronal cell bodies filled with a grossly enlarged vacuole and/or missing cell bodies from neural cells that had formed and degenerated. Because the overall shape and size of the brain was normal, it appears that Vac14 is not required for early neural development.

In the peripheral nervous system, for example, the trigeminal ganglion and dorsal root ganglion, the cell bodies from mutant mice frequently contained vacuoles (Fig. 2*b*). The degree of vacuolation ranged from multiple small cytoplasmic vacuoles to a single, large vacuole that filled the entire cell body. Similar defects were observed in the brains of Vac14$^{\beta\text{-geo}/\beta\text{-geo}}$ embryonic day (E)18 embryos (data not shown). The nervous systems of

both Vac14$^{+/+}$ and heterozygous Vac14$^{+/\beta\text{-geo}}$ E18 embryos and P0 pups appeared normal.

The holes observed in the brains of the Vac14$^{\beta\text{-geo}/\beta\text{-geo}}$ mice suggested that there might be a significant increase in cell death. Therefore, we surveyed the levels of apoptotic cells in the brains from three pairs of mutant P0 pups and corresponding wild-type littermates. A series of 40-μm coronal sections were prepared from the entire brain. Starting 80 μm rostral to the crossing of the corpus callosum every third section was immunostained by using an antibody for activated caspase-3, a common marker for apoptotic cells. All sections of Vac14$^{\beta\text{-geo}/\beta\text{-geo}}$ mice were comparable in size with their wild-type littermates; however, two of the three mutant brains had enlarged lateral ventricles. Two confined regions within the forebrains of Vac14$^{\beta\text{-geo}/\beta\text{-geo}}$ mice had significantly increased levels of apoptotic cells (SI Fig. 8). A region of the septum immediately caudal to the corpus callosum showed a high number of activated caspase-3-positive cells; few positive cells were observed in corresponding sections from the same region of brains from littermate controls (SI Fig. 8*a*). Increased apoptosis was also found in the cingulate cortex (SI Fig. 8*b*). The highest increase in apoptosis occurred in the midbrain and hindbrain, particularly in regions where we observed the lesions in H&E-stained sections. Although both mutant and wild-type brains had cells with activated caspase-3 scattered throughout these regions, the Vac14$^{\beta\text{-geo}/\beta\text{-geo}}$ mice had clusters of apoptotic cells in multiple confined areas. An example occurs in the beginning of the midbrain, 400 μm caudal to the beginning of the posterior commissure (SI Fig. 9).

Despite the fact that Vac14 and Fab1 are present in all tissues, the only obvious defects in the Vac14$^{\beta\text{-geo}/\beta\text{-geo}}$ P0 pups were observed in the nervous system. The spleen, liver, kidney, lung, heart, and intestine appeared normal in size, cellularity, and architecture (SI Fig. 7*b* and data not shown).

Although Vac14$^{\beta\text{-geo}/\beta\text{-geo}}$ hippocampal and cortical neurons appeared normal *in vivo*, these neurons formed vacuoles in culture (Fig. 3*a*) (n = 50). Vacuoles were not observed in neurons cultured from wild-type mice. Neurite outgrowth appeared normal in both the mutant and wild-type neurons.

Although large holes were not observed in other tissues *in vivo*, it is likely that other cell types have the potential to form vacuoles. Examination of fibroblasts cultured from P0 Vac14$^{\beta\text{-geo}/\beta\text{-geo}}$ mice revealed cells with multiple, large vacuoles. Although morphologically similar to lipid droplets in adipocytes, they are not labeled by the lipophilic dye Nile red (SI Fig. 10). The vacuoles appear to be due to the loss of Vac14 function. Wild-type and Vac14$^{\beta\text{-geo}/\beta\text{-geo}}$ fibroblasts were electroporated with a cDNA encoding human Vac14 fused to citrine [mCit (19, 20)], a variant of yellow fluorescent protein (YFP), or an mCit-only control. Before electroporation, a high percentage (>80%) of Vac14$^{\beta\text{-geo}/\beta\text{-geo}}$ fibroblasts were vacuolated. Subplating confluent mutant fibroblasts with or without electroporation resulted in a transient decline in the percentage of cells with enlarged vacuoles (data not shown). Six hours after transfection, the percentage of Vac14$^{\beta\text{-geo}/\beta\text{-geo}}$ cells with vacuoles was 2-fold lower in those with Vac14-mCit, than in those with mCit alone (Fig. 3*b*). This difference increased with time. Twenty-four hours after electroporation, most cells transfected with Vac14-mCit were devoid of vacuoles, whereas the number of mCit-transfected cells with vacuoles rose to ≈80%. Note that in the presence of Vac14-mCit, previously formed vacuoles disappeared, and suppression of newly formed vacuoles occurred as well. These results strongly suggest that vacuolation is due to the loss of Vac14.

Vac14 is an activator of Fab1 in yeast. The lowered levels of PI(3,5)P_2 and PI(5)P in mouse fibroblasts indicate that Vac14 is an activator of Fab1/PIKfyve in mice as well. To directly test whether the vacuoles observed in Vac14$^{\beta\text{-geo}/\beta\text{-geo}}$ mice are due to diminished Fab1/PIKfyve activity or an as yet unknown function of Vac14, we overexpressed human Fab1-mCit in Vac14$^{\beta\text{-geo}/\beta\text{-geo}}$ fibroblasts. Notably, the expression of Fab1-mCit resulted in the disappearance of previously formed vacuoles and strongly suppressed the formation of new vacuoles (Fig. 3*b*). These results are consistent with the postulate that, as in yeast, the major function of Vac14 in mammals is the regulation of PI(3,5)P_2 and its related metabolites.

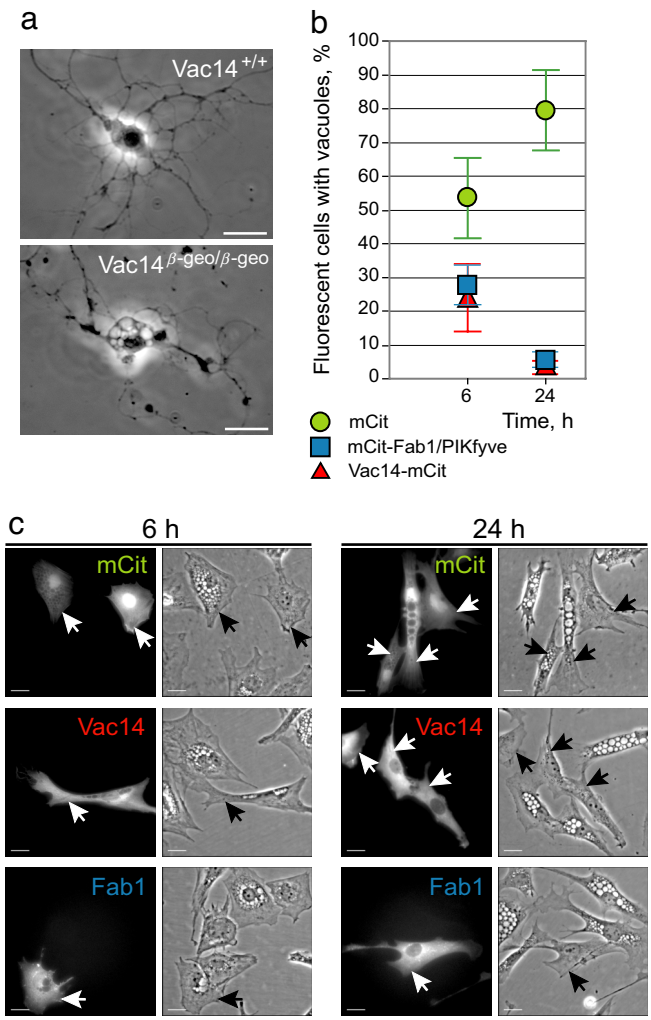

Fig. 3. Expression of Vac14-mCit and overexpression of mCit-Fab1/PIKfyve in Vac14$^{\beta\text{-geo}/\beta\text{-geo}}$ fibroblasts leads to the suppression of vacuole formation. (*a*) Vacuolation occurs in neuronal primary cultures. Cortices were dissected from E16.5 embryos and cultured for 2 weeks. Images of live cells were taken on a Nikon TE-2000 inverted microscope with a ×40 phase-contrast objective. (Scale bars, 20 μm.) (*b*) Cells were transfected with the indicated plasmids. Fluorescent cells were scored for the presence of vacuoles. Each data point is a mean of four independent experiments. For each experiment >100 cells were counted. Error bars represent SD. (*c*) Representative cells for 6 and 24 h after transfection are shown. Arrows indicate transfected cells.

To determine whether these large vacuoles are predominantly due to macropinocytosis or whether they arise from internal membranes, we made time-lapse movies of individual fibroblasts. In both mutant and wild-type fibroblasts (SI Movies 1 and 2), vacuoles arose that were due to macropinocytosis. These vacuoles appeared in regions of the plasma membrane coincident with ruffling filopodia. The newly formed vacuoles then rapidly moved inward to regions adjacent to the nucleus and rapidly disappeared (SI Movies 1 and 2). In the mutant, of 31 cells observed, in 13 examples, massive macropinocytosis occurred; in each case the macropinosomes resolved in a wild-type time frame (SI Movie 2). In all seven examples, where vacuoles

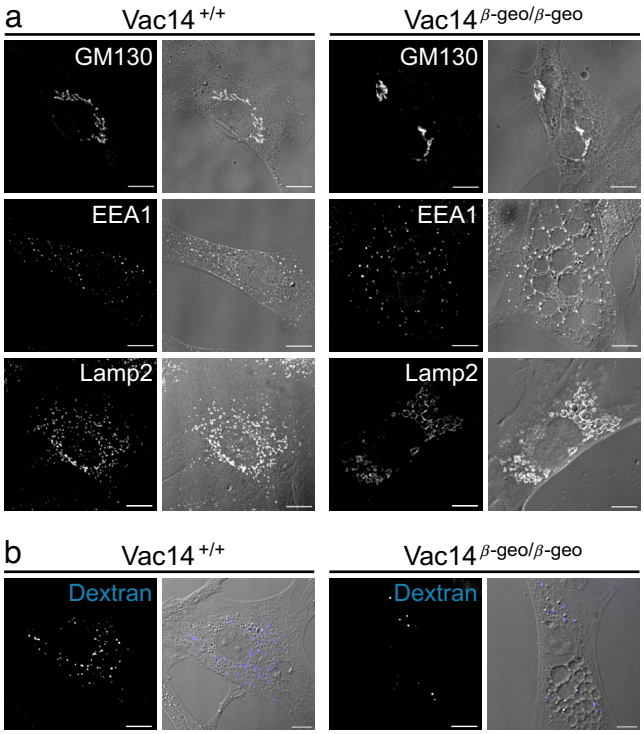

Fig. 4. Vacuoles appear to form from late endosomes/lysosomes. (*a*) Primary fibroblasts were labeled with GM130 (Golgi marker), EEA1 (early endosome marker), or Lamp2 (late endosome and lysosome marker). Although the *cis*-Golgi appears normal in Vac14$^{\beta\text{-geo}/\beta\text{-geo}}$ cells, early endosomes are frequently enlarged. The limiting membrane of the vacuoles in Vac14$^{\beta\text{-geo}/\beta\text{-geo}}$ cells is labeled with Lamp2. (*b*) Vacuoles in Vac14$^{\beta\text{-geo}/\beta\text{-geo}}$ cells are incapable of receiving fluid phase marker dextran. Vac14$^{+/+}$ and Vac14$^{\beta\text{-geo}/\beta\text{-geo}}$ fibroblasts were incubated with dextran Cascade blue for 16 h and chased for 2 h. (Scale bars, 10 μm.)

arose and persisted, their origin was unclear (SI Movie 3). This event was not observed in any of the 21 wild-type cells examined.

Vac14 and Fab1 colocalize with each other in yeast (9) and in mammalian cells (21). Fab1/PIKfyve had been reported to localize to late endosomes (22), whereas a recent study showed colocalization with the early endosome (23). In the mammalian studies, exogenously expressed tagged proteins were used. The antiserum raised to Vac14 in this study was not suitable for immunofluorescence. Although there is ambiguity concerning the precise location of Vac14, based on its association with PIKfyve/Fab1, it is likely that it localizes to endosomal structures.

To test which organelles are affected by loss of Vac14 and to identify the origin of the Vac14$^{\beta\text{-geo}/\beta\text{-geo}}$-related vacuoles, we tested the localization of selected organellar proteins (Fig. 4*a*). The Golgi, labeled by GM130, exhibited a typical perinuclear tubular pattern in both Vac14$^{+/+}$ and Vac14$^{\beta\text{-geo}/\beta\text{-geo}}$ cells. Early endosomes, labeled by EEA1, were slightly enlarged in Vac14$^{\beta\text{-geo}/\beta\text{-geo}}$ fibroblasts, suggesting a possible defect in early endosomal organelles. Note that EEA1 was not detected on the vacuole membranes, suggesting that the vacuoles are not derived from early endosomes. In contrast, the limiting membranes of the vacuoles were labeled with Lamp2, a marker of late endosomes and lysosomes. These results strongly suggest that vacuoles arise because of swelling of either or both of these organelles. In addition to vacuoles, Lamp2-positive dots were observed. These likely represent normal late endosomes and lysosomes.

We monitored fluid-phase endocytosis to test whether the vacuoles observed in Vac14$^{\beta\text{-geo}/\beta\text{-geo}}$ fibroblasts remain a functional part of the endocytic pathway. Cells were incubated with Cascade blue dextran for a 16-hour pulse, followed by a 2-hour chase, to allow the dextran to accumulate in lysosomes. The fluid phase marker was taken up by Vac14$^{\beta\text{-geo}/\beta\text{-geo}}$ fibroblasts; punctate dots were found in both mutant and wild-type cells (Fig. 4*b*). However, dextran was not detected in the vacuoles. This finding strongly suggests that the vacuoles are not part of the normal endocytic pathway. A similar defect was observed in cells expressing dominant-negative Fab1/PIKfyve (24).

Receptor-mediated endocytosis is not affected by loss of Vac14. After starvation and stimulation with EGF, total EGFR levels in the cell were analyzed at several time points by Western blot analysis. Three independent pairs of Vac14$^{+/+}$ and Vac14$^{\beta\text{-geo}/\beta\text{-geo}}$ cells were compared (SI Fig. 11). No significant differences were observed. This suggests that, in the absence of Vac14, EGFR is still efficiently transported to lysosomes.

The steady-state localization of the cation-independent mannose-6-phosphate receptor (CI-MPR) is perturbed in Vac14$^{\beta\text{-geo}/\beta\text{-geo}}$ fibroblasts. CI-MRP cycles between the trans-Golgi network (TGN) and endosomes. In most cell types, CI-MPR is found predominantly in the TGN, and thus is concentrated in a perinuclear region of the cell. This same localization was observed in Vac14$^{+/+}$ fibroblasts. In contrast, in Vac14$^{\beta\text{-geo}/\beta\text{-geo}}$ fibroblasts CI-MPR was found in small spots and enlarged vesicles that were dispersed in the cytoplasm (Fig. 5*a*). Some of the vesicles were EEA1 or Lamp2-positive, suggesting that, in Vac14$^{\beta\text{-geo}/\beta\text{-geo}}$ fibroblasts, there is a defect in retrograde traffic of CI-MPR from late and early endosomes back to the TGN. Consistent with this hypothesis, we observed a defect in the trafficking of cathepsin D, one of the enzymes transported by CI-MPR. Normally, newly synthesized procathepsin D is transported by CI-MPR from the TGN to endosomes, where the propeptide is cleaved, giving rise to intermediate forms. These intermediate forms are transported to the lysosome and further cleaved into two noncovalently linked fragments. Western blot analysis of cathepsin D revealed that both the pro- and intermediate forms accumulated in Vac14$^{\beta\text{-geo}/\beta\text{-geo}}$ cells (Fig. 5*b*). The accumulation of procathepsin D is consistent with a lack of CI-MRP in the TGN. A similar defect was observed in siRNA-mediated knockdown of Fab1/PIKfyve (23).

Accumulation of the intermediate form of cathepsin D suggests that there might also be a delay in the transition of late endosomes to lysosomes. This latter defect and the fact that the swollen Lamp2-positive vacuoles cannot receive fluid-phase markers are consistent with the hypothesis that loss of Vac14 causes defects in some late endosomal functions.

Discussion

Phosphatidylinositol polyphosphates regulate diverse functions, and defects in their metabolism likely contribute to many human diseases (25). Here, we analyzed a mouse model with undetectable Vac14 protein levels and find that loss of Vac14 leads to a 57% decrease in the levels of PI(3,5)P_2, a 45% decrease in the levels of PI(5)P, and a 2.4-fold increase in the levels of PI(3)P. The mice die perinatally and exhibit profound degeneration in certain regions of the central and peripheral nervous systems. Selected regions in the brain are affected, especially the medulla, the pons, and the midbrain. Increased cell death occurs in these areas. Affected neurons contain large vacuoles, and vacuoles also arise in both neurons and fibroblasts cultured from the mutant mice.

The finding that the enlarged vacuoles in cells from the Vac14$^{\beta\text{-geo}/\beta\text{-geo}}$ mice contain markers of the late endosome is consistent with several other studies. Large vacuoles that contain late endosomal markers occur because of overexpression of dominant-negative Fab1/PIKfvye (26) or depletion of Fab1/PIKfyve by siRNA (23). They are observed in mice with a null mutation of the PI(3,5)P_2 5-phosphatase Fig4 (33), and in *Caenorhabditis elegans* (27) and *Drosophilia* (28) with mutations

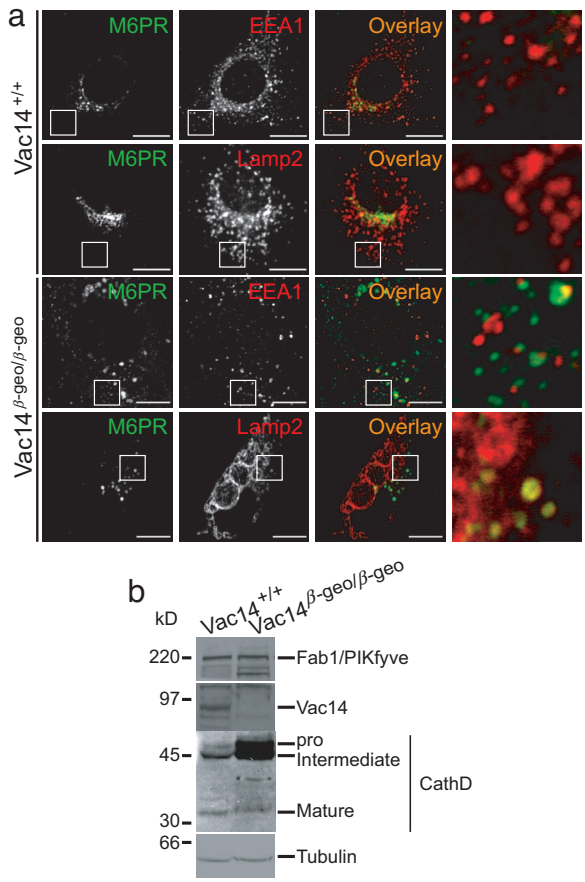

Fig. 5. Endosome-to-TGN trafficking is defective in Vac14$^{\beta\text{-geo}/\beta\text{-geo}}$ fibroblasts. (*a*) CI-MPR is trapped in a mixed population of endosomes. Vac14$^{+/+}$ and Vac14$^{\beta\text{-geo}/\beta\text{-geo}}$ fibroblasts were fixed as above and double labeled with CI-MPR (green) and EEA1 or Lamp2 (red). Images were taken on a Zeiss confocal microscope. Peripheral regions of cells marked by squares are shown in an amplified view. (*b*) Pro- and intermediate cathepsin D accumulate in Vac14$^{\beta\text{-geo}/\beta\text{-geo}}$ fibroblasts. Steady-state levels of cathepsin D in whole-cell lysates from Vac14$^{+/+}$ and Vac14$^{\beta\text{-geo}/\beta\text{-geo}}$ fibroblasts were analyzed by Western blot.

in Fab1/PIKfyve. Moreover, large vacuoles are observed in *fab1*Δ and *vac14*Δ yeast mutants (7, 11).

That these large vacuoles have late endosomal markers and that PI(3,5)P_2 is required for the retrograde transport from late endosomes to the TGN (ref. 23 and this study) and also for sorting a subset of cargoes into the lumen of multivesicular bodies (8, 29–31), strongly suggests that the large vacuoles arise from late endosomes and occur because of defects in membrane traffic from the late endosome.

The enlarged vacuoles are likely because of lowered levels of PI(3,5)P_2 rather than elevation of PI(3)P. siRNA knockdown of Vps34, the PI(3)-kinase that produces the PI(3)P substrate used by Fab1 causes lowered levels of both PI(3)P and PI(3,5)P_2 and results in large vacuoles that contain late endosomal markers (32).

It is also unlikely that lowered levels of PI(5)P cause the enlarged vacuoles. Mutations in myotubularins, which are predicted to lower PI(5)P levels, have not been found to produce large vacuoles.

The spontaneous mouse mutant, *pale tremor*, has a loss of function mutation in the Fig4 gene (33). We recently showed that, in addition to its lipid phosphatase activity in the conversion of PI(3,5)P_2 to PI3P, Fig4 has a second opposing function and is required for the production of PI(3,5)P_2. In yeast, Vac14 and Fig4 act in the same pathway, form a complex with each other, and each knockout strain, *vac14*Δ and *Fig4*Δ, has a partial loss of PI(3,5)P_2 (4, 7–9, 11). Our recent studies suggest that Fig4 serves the same dual role in mammals. Cells cultured from the Fig4 mutant mouse have significantly reduced PI(3,5)P_2 (33).

Importantly, the Fig4 and Vac14 mouse mutants have similar defects in levels of PI(3,5)P_2, and acquire profound vacuolation in the same types of neurons. The similar pattern of neurodegeneration strongly supports the hypothesis that the neurodegeneration observed in both mice is a direct consequence of defects in the metabolism of PI(3,5)P_2 and/or PI(5)P. Moreover, human mutations of *Fig4* result in the peripheral nerve disorder Charcot–Marie–Tooth syndrome (CMT4J) (1). This finding strongly suggests that mutations in Vac14 and Fab1/PIKfyve could result in Charcot–Marie–Tooth synddrome as well as other neurological disorders.

Mutations in myotubularin-related genes, which are predicted to have reduced levels of PI(5)P, also cause neuropathic diseases in mice and humans (34–36), but these defects are distinct from the defects observed in the Vac14 or Fig4 mouse mutants. The neurological defects are not as severe, vacuolation does not occur, and the myotubularin mutations are not lethal.

Mutations in proteins that regulate other phosphoinositides have been shown to lead to neurological defects (37–40). None of these genes is known to affect levels of PI(3,5)P_2, and the phenotypes are distinct from those observed in the Vac14 or Fig4 mice.

Although Vac14 has a wide tissue distribution, neurons are particularly sensitive to reduction of PI(3,5)P_2. This may be due to the presence of extraordinarily long processes in the affected neurons. Alternatively, PI(3,5)P_2 may play a critical role in an as yet unidentified neuronal-specific endosomally derived organelle. Indeed, during subcellular fractionation of rat brain, Vac14 was enriched in microsomal membranes from synapses (41).

The finding that loss of PI(3,5)P_2 leads to neurodegeneration may be directly linked to recent discoveries that some forms of Alzheimer's disease correlate with defects in SORL1 (42) and Vps35 (43), which function in the same pathway. Vps35 is part of the retromer complex and in humans is required to form tubular carriers from the endosomes that travel by retrograde traffic to the trans-Golgi network (reviewed in ref. 44). Notably, fibroblasts from the Vac14$^{\beta\text{-geo}/\beta\text{-geo}}$ mice show a defect in this pathway. Thus, loss of PI(3,5)P_2 in neurons may be particularly deleterious because of subsequent defects in membrane traffic from endosomes to the TGN.

The discovery that PI(3,5)P_2 is critical to neuronal health may lead to a molecular understanding of some forms of neurodegeneration and will hopefully lead to new therapeutic approaches to treat these serious diseases.

Materials and Methods

HPLC. For separation of glycerophosphoinositides, two elution gradients were used at 1 ml/min flow rate. (pump A: H_2O; pump B: 1M $(NH_4)_2HPO_4$, pH3.8). Gradient 1: 0% B 5 min; 0–2% B 15 min; 2% B 80 min; 2–12% B 20 min; 12% B 20 min; 12–80% B 40 min; 80% B 20 min; 80–0% B 5 min. Gradient 2 (to separate GroPIns(3,4)P_2 from GroPIns(3,5)P_2): 0% B 5 min; 0–2% B 15 min; 2% B 80 min; 2–10% B 20 min; 10% B 65 min; 10–80% B 40 min; 80% B 20 min; 80–0% B 5 min. Positions of GroPIns(3)P, GroPIns(3,5)P_2, GroPIns(3,4)P_2 and GroPIns(3,4,5)P_3 determined by ^{32}P-labeled standards were received as gifts from Lucia Rameh (Biomedical Research Institute, Boston, MA). Positions of GroPIns(4)P and GroPIns(4,5)P_2 were confirmed with yeast glycerophosphoinositide extracts (4). Position of GroPIns(5)P was based on its migration relative to GroPIns(4)P (13, 45). The elution position of GroPIns(5)P is close to that of GroPIns(4)P; the shoulder of GroPIns(4)P overlapped GroPIns(5)P. For GroPIns(5)P, we

quantified the right half of the GroPIns(5)P peak and estimated the total using a factor of 2. In Vac14$^{\beta\text{-geo}/\beta\text{-geo}}$ where no peak was seen, we integrated the values from the same elution position as the latter half of GroPIns(5)P peak and multiplied by a factor of 2.

All experiments were performed in compliance with the guidelines of the University Committee on Use and Care of Animals of the University of Michigan. Animals were housed and cared for in accordance with National Institutes of Health guidelines.

Generation of Mice, Antibodies, Inositol Labeling, Western Blot, Primary Fibroblast and Neuron Cultures, Histology, Immunofluorescence, Immunohistochemistry, Dextran Uptake, Nile Red Staining, Electroporation, EGFR Degradation, and Live-Cell Imaging. See *SI Materials and Methods* for detailed experimental procedures for generation of the mice, antibodies, inositol labeling, Western blot, primary fibroblast and neuron cultures, histology, immunofluorescence, immunohistochemistry, dextran uptake, Nile red staining, electroporation, EGFR degradation, and live-cell imaging.

We thank Drs. James Dowling, David Ginsburg, Jason Gestwicki, and John Stokes for helpful discussions; Drs. Kristen Verhey and Jennetta Hammond for help with culturing primary neurons; and Dr. Nancy L. Lill for help with the EGFR degradation assay. The mAb for LAMP-2 was developed by Dr. Thomas August and provided by the Developmental Studies Hybridoma Bank (developed under the auspices of the National Institute of Child Health and Human Development and maintained by the Department of Biological Sciences, University of Iowa). This work was supported by National Institutes of Health Grants R01 GM50403 (to L.S.W.) and R01 GM24872 (to M.H.M.). Generation of the Vac14$^{\beta\text{-geo}/\beta\text{-geo}}$ mouse was supported in part by Pilot Grant P50 DK52617 from the O'Brien Kidney Research Center, University of Iowa. C.Y.C. was supported by Genetics Predoctoral Training Grant NIH-T32 GM07544. S.C.R. was supported by Engineering and Physical Sciences Research Council (EP/C013220/1) and the American Heart Association (0120475Z and 0325605Z).

1. Whiteford CC, Brearley CA, Ulug ET (1997) *Biochem J* 323(Pt 3):597–601.
2. Dove SK, Cooke FT, Douglas MR, Sayers LG, Parker PJ, Michell RH (1997) *Nature* 390:187–192.
3. Rameh LE, Tolias KF, Duckworth BC, Cantley LC (1997) *Nature* 390:192–196.
4. Duex JE, Tang F, Weisman LS (2006) *J Cell Biol* 172:693–704.
5. Gary JD, Wurmser AE, Bonangelino CJ, Weisman LS, Emr SD (1998) *J Cell Biol* 143:65–79.
6. McEwen RK, Dove SK, Cooke FT, Painter GF, Holmes AB, Shisheva A, Ohya Y, Parker PJ, Michell RH (1999) *J Biol Chem* 274:33905–33912.
7. Bonangelino CJ, Nau JJ, Duex JE, Brinkman M, Wurmser AE, Gary JD, Emr SD, Weisman LS (2002) *J Cell Biol* 156:1015–1028.
8. Dove SK, McEwen RK, Mayes A, Hughes DC, Beggs JD, Michell RH (2002) *Curr Biol* 12:885–893.
9. Duex JE, Nau JJ, Kauffman EJ, Weisman LS (2006) *Eukaryot Cell* 5:723–731.
10. Rudge SA, Anderson DM, Emr SD (2004) *Mol Biol Cell* 15:24–36.
11. Gary JD, Sato TK, Stefan CJ, Bonangelino CJ, Weisman LS, Emr SD (2002) *Mol Biol Cell* 13:1238–1251.
12. Walker DM, Urbe S, Dove SK, Tenza D, Raposo G, Clague MJ (2001) *Curr Biol* 11:1600–1605.
13. Schaletzky J, Dove SK, Short B, Lorenzo O, Clague MJ, Barr FA (2003) *Curr Biol* 13:504–509.
14. Tronchere H, Laporte J, Pendaries C, Chaussade C, Liaubet L, Pirola L, Mandel JL, Payrastre B (2004) *J Biol Chem* 279:7304–7312.
15. Tosch V, Rohde HM, Tronchere H, Zanoteli E, Monroy N, Kretz C, Dondaine N, Payrastre B, Mandel JL, Laporte J (2006) *Hum Mol Genet* 15:3098–3106.
16. Sbrissa D, Ikonomov OC, Deeb R, Shisheva A (2002) *J Biol Chem* 277:47276–47284.
17. Li S, Tiab L, Jiao X, Munier FL, Zografos L, Frueh BE, Sergeev Y, Smith J, Rubin B, Meallet MA, *et al.* (2005) *Am J Hum Genet* 77:54–63.
18. Hawkins PT, Jackson TR, Stephens LR (1992) *Nature* 358:157–159.
19. Griesbeck O, Baird GS, Campbell RE, Zacharias DA, Tsien RY (2001) *J Biol Chem* 276:29188–29194.
20. Zhang J, Campbell RE, Ting AY, Tsien RY (2002) *Nat Rev Mol Cell Biol* 3:906–918.
21. Sbrissa D, Ikonomov OC, Strakova J, Dondapati R, Mlak K, Deeb R, Silver R, Shisheva A (2004) *Mol Cell Biol* 24:10437–10447.
22. Ikonomov OC, Sbrissa D, Shisheva A (2001) *J Biol Chem* 276:26141–26147.
23. Rutherford AC, Traer C, Wassmer T, Pattni K, Bujny MV, Carlton JG, Stenmark H, Cullen PJ (2006) *J Cell Sci* 119:3944–3957.
24. Ikonomov OC, Sbrissa D, Foti M, Carpentier J-L, Shisheva A (2003) *Mol Biol Cell* 14:4581–4591.
25. Pendaries C, Tronchere H, Plantavid M, Payrastre B (2003) *FEBS Lett* 546:25–31.
26. Ikonomov OC, Sbrissa D, Mlak K, Kanzaki M, Pessin J, Shisheva A (2002) *J Biol Chem* 277:9206–9211.
27. Nicot AS, Fares H, Payrastre B, Chisholm AD, Labouesse M, Laporte J (2006) *Mol Biol Cell* 17:3062–3074.
28. Rusten TE, Rodahl LM, Pattni K, Englund C, Samakovlis C, Dove S, Brech A, Stenmark H (2006) *Mol Biol Cell* 17:3989–4001.
29. Odorizzi G, Babst M, Emr SD (1998) *Cell* 95:847–858.
30. Reggiori F, Pelham HRB (2002) *Nat Cell Biol* 4:117–123.
31. Shaw JD, Hama H, Sohrabi F, DeWald DB, Wendland B (2003) *Traffic* 4:479–490.
32. Johnson EE, Overmeyer JH, Gunning WT, Maltese WA (2006) *J Cell Sci* 119:1219–1232.
33. Chow CY, Zhang Y, Dowling JJ, Jin N, Adamska M, Shiga K, Szigeti K, Shy ME, Li J, Zhang X, *et al.* (2007) *Nature* 448:68–72.
34. Bolino A, Muglia M, Conforti FL, LeGuern E, Salih MA, Georgiou DM, Christodoulou K, Hausmanowa-Petrusewicz I, Mandich P, Schenone A, *et al.* (2000) *Nat Genet* 25:17–19.
35. Bolino A, Bolis A, Previtali SC, Dina G, Bussini S, Dati G, Amadio S, Del Carro U, Mruk DD, Feltri ML, *et al.* (2004) *J Cell Biol* 167:711–721.
36. Bonneick S, Boentert M, Berger P, Atanasoski S, Mantei N, Wessig C, Toyka KV, Young P, Suter U (2005) *Hum Mol Genet* 14:3685–3695.
37. Cremona O, Di Paolo G, Wenk MR, Luthi A, Kim WT, Takei K, Daniell L, Nemoto Y, Shears SB, Flavell RA, *et al.* (1999) *Cell* 99:179–188.
38. Di Paolo G, Moskowitz HS, Gipson K, Wenk MR, Voronov S, Obayashi M, Flavell R, Fitzsimonds RM, Ryan TA, De Camilli P (2004) *Nature* 431:415–422.
39. Lowe M (2005) *Traffic* 6:711–719.
40. Nystuen A, Legare ME, Shultz LD, Frankel WN (2001) *Neuron* 32:203–212.
41. Lemaire JF, McPherson PS (2006) *FEBS Lett* 580:6948–6954.
42. Rogaeva E, Meng Y, Lee JH, Gu Y, Kawarai T, Zou F, Katayama T, Baldwin CT, Cheng R, Hasegawa H, *et al.* (2007) *Nat Genet* 39:168–177.
43. Small SA, Kent K, Pierce A, Leung C, Kang MS, Okada H, Honig L, Vonsattel JP, Kim TW (2005) *Ann Neurol* 58:909–919.
44. Bonifacino JS, Rojas R (2006) *Nat Rev Mol Cell Biol* 7:568–579.
45. Tolias KF, Rameh LE, Ishihara H, Shibasaki Y, Chen J, Prestwich GD, Cantley LC, Carpenter CL (1998) *J Biol Chem* 273:18040–18046.